RP105 protects PC12 cells from oxygen-glucose deprivation/reoxygenation injury via activation of the PI3K/AKT signaling pathway

YANPENG SUN, LU LIU, JIANG YUAN, QIANG SUN, NA WANG and YUNFU WANG

Department of Neurology, Taihe Hospital, Hubei University of Medicine, Shiyan, Hubei 442000, P.R. China

Received August 27, 2017; Accepted January 10, 2018

DOI: 10.3892/ijmm.2018.3482

Abstract. Radioprotective 105 kDa protein (RP105) has been reported to produce favorable outcomes in various cardiovascular disorders via a toll-like receptor 4-dependent or -independent manner. However, whether RP105 exerts neuroprotective effects against oxygen-glucose deprivation (OGD)/reoxygenation (OGD/R) injury remains to be elucidated. In the present study, the PC12 neuronal cell line was exposed to 4 h of OGD followed by 24 h of reoxygenation. Adenoviral vectors encoding RP105 were utilized to upregulate the level of RP105 in PC12 cells prior to OGD/R induction. The results demonstrated that OGD/R reduced the expression of RP105 at the mRNA and protein levels. The overexpression of RP105 significantly reversed OGD/R-induced neuronal injuries, as demonstrated by the reduced release of lactate dehydrogenate and enhanced cellular viability, in addition to decreased inflammation, apoptosis and reactive oxygen species. The mechanistic evaluations indicated that the neuroprotective functions of RP105 were, in part, a result of activation of the phosphatidylinositol 3-kinase (PI3K)/protein kinase B (AKT) pathway. In addition, elimination of the PI3K/AKT axis via the use of a pharmacological inhibitor inhibited the OGD/R-inhibitory effects induced by the overexpression of RP105. Taken together, RP105 protected PC12 cells from OGD/R injury through promotion of the PI3K/AKT pathway; therefore, the RP105-PI3K-AKT axis may provide a novel therapeutic target for the prevention of cerebral ischemia/reperfusion injury.

Correspondence to: Dr Yunfu Wang, Department of Neurology, Taihe Hospital, Hubei University of Medicine, 32 South Renmin Road, Shiyan, Hubei 442000, P.R. China
E-mail: sunyptaihe@163.com

Abbreviations: RP105, radioprotective 105 kDa protein; OGD/R, oxygen-glucose deprivation/reoxygenation; I/R, ischemia/reperfusion; PI3K, phosphatidylinositol 3-kinase; AKT, protein kinase B

Key words: radioprotective 105 kDa protein, oxygen-glucose deprivation/reoxygenation, phosphatidylinositol 3-kinase, protein kinase B

Introduction

The consequences of blood deprivation have been commonly acknowledged as important concerns in the clinical manifestations of myocardial infarction, stroke and shock (1,2). The restoration of blood flow is crucial to prevent irreversible neuron death, with reperfusion leading to augmented inflammation, apoptosis and reactive oxygen species (ROS), in excess of that triggered by ischemia alone (1,2). The pathogenesis and interventional options for cerebral ischemia/reperfusion (I/R) injury have been expanded and derived form a series of experimental observations, although these advances have yet to be fully integrated into clinical practices (1-3). According to the concept that cerebral I/R injury involves complex pathophysiological processes, increasing investigations aimed at elucidating the interferences of multiple etiologies may provide promising approaches to minimize the detrimental effects of cerebral I/R injury.

Transmembrane receptors, particularly for radioprotective 105 kDa protein (RP105) and toll-like receptor 4 (TLR4), function as bridges by sensing extracellular stimuli and thereby transferring signals to intercellular effectors (4-6). In this manner, they may be implicated in neuronal injury in response to I/R or oxygen-glucose deprivation/reoxygenation (OGD/R) insult with respect to inflammation, apoptosis and ROS (7,8). RP105 is a member of the TLR family and acts as an endogenous inhibitor of TLR4, regulating acute/chronic myocardial ischemia and pressure overload-induced cardiac remodeling (9-11). Although the benefits have been well established for RP105 with regard to dependence on TLR4-limited patterns, data since has shown the effects of RP105 in TLR4-independent approaches (10). The phosphoinositide 3-kinase (PI3K) and serine/threonine kinase, protein kinase B (AKT) signaling pathways have been suggested as potent downstream effectors of RP105 under I/R stimulation and the immune response (10,12). In terms of their functional and physical connections, the fundamental detection of RP105 and the PI3K/AKT pathway in cerebral I/R injury have generated substantial interest.

Substantial evidence has indicated that the activity of the PI3K/AKT pathway exerts neuroprotective effects against I/R injury, which is reinforced by the inhibition of PI3K/AKT driving the progression of I/R (13). Due to the potential of

PI3K/AKT signaling as a substrate of RP105, it is of interest to examine the existence of an RP105-PI3K-AKT axis in cerebral I/R, whereby RP105 exerts pleiotropic protective functions. In the present study, it was demonstrated that the OGD/R-induced impairment of PC12 cells was markedly ameliorated by the overexpression of RP105, as exhibited by weakened lactate dehydrogenase (LDH) release, reductions in inflammation, ROS and apoptosis, and increased cellular viability. The mechanistic estimations revealed that the favorable RP105-induced effects on OGD/R were due, in part, to the activation of the PI3K/AKT pathways, and elimination of the PI3K/AKT axis inhibited the inhibitory potency of RP105 on OGD/R. These results indicated that RP105 may be a potent therapeutic candidate for the prevention of cerebral I/R.

Materials and methods

Cell incubation and adenoviral vector transfection. The PC12 cells (American Type Cell Culture Collections, Manassas, VA, USA) were cultured in Dulbecco's modified Eagle's medium (DMEM; Gibco; Thermo Fisher Scientific, Inc., Waltham, MA, USA) supplemented with 10% fetal bovine serum (FBS; Gibco; Thermo Fisher Scientific, Inc.) and 1% penicillin/streptomycin in a humidified atmosphere at 37˚C with 5% CO_2 and 95% air (2). The cells were seeded into microplates at a suitable density, satisfying each experimental protocol, and the medium was replaced every 24 h.

Adenoviruses encoding RP105 (Ad-RP105) or GFP (Ad-GFP) as a control were provided by GenePharma Company (Shanghai, China) with the viral titer at $1.5x10^{10}$ PFU/ml. For viral transduction, the PC12 cells were incubated at 37˚C with Ad-RP105 or Ad-GFP at different multiplicities of infections (MOI) for 4 h. An MOI of 50 was used in the subsequent experiments due to its ~95% transduction efficiency and no significant effect on cellular viability. At 48 h post-transduction, the cells were subjected to OGD/R treatment (14,15). Each experiment was performed in triplicate.

OGD/R establishment and experimental design. Following 48 h of adenoviral transduction, the PC12 cells underwent OGD/R treatment according to a prior demonstration with minor modifications (16). In detail, the cells were washed twice with glucose-free Earle's balanced salt solution, and maintained in pre-warmed (37˚C) glucose-free DMEM without FBS. Subsequently, the cells were transferred into an oxygen-deprived incubator (5% CO_2 and 95% N_2) at 37˚C for 4 h. Reoxygenation was initiated by exposing the cells to normal medium and maintaining the cells in a normal incubator for another 24 h.

To examine the potential function of RP105 in PC12 cells during OGD/R injury, the cells were divided into four groups: i) Control group, cells were cultured in normal medium in a normal incubator; ii) OGD/R group, cells underwent 4 h of OGD followed by 24 h reoxygenation; iii) Ad-GFP+OGD/R, cells were transduced with Ad-GFP and underwent OGD/R; iv) Ad-RP105+OGD/R, cells were transduced with Ad-RP105 and then subjected to OGD/R. To estimate the potential molecular mechanisms of RP105 in PC12 cells under the OGD/R condition, the virus-transduced PC12 cells at a density of $1x10^6$ cells/6-well plate were incubated at 37˚C with or without 10 μM LY294002 for 1 h, a specific PI3K inhibitor (Sigma-Aldrich; Merck Millipore, Darmstadt, Germany), prior to the OGD/R establishment.

Biochemical analysis. Following OGD/R treatment, the supernatants of the cultured PC12 cells were collected for biological analysis of LDH, a well-regarded marker of neuronal death (2). The supernatant was immediately centrifuged at 1,370 x g for 5 min at 4˚C, and was subjected to commercial kits using standard protocols (Nanjing Jiancheng Bioengineering Institute, Nanjing, China) according to the manufacturer (2). The results were determined in international units per liter.

Cell Counting Kit (CCK)-8 assays. A CCK-8 assay was performed to quantitatively detect cell survival according to a previous method (2). The PC12 cells were seeded into 96-well plates at a density of $6x10^3$ cells/well for 24 h of incubation. Following the experimental procedures, 20 μl of CCK-8 reagent (Dojindo Molecular Laboratories, Inc., Kumamoto, Japan) was added into each well, followed by continuous incubation at 37˚C for 4 h. The optical density values were measured with a microplate spectrophotometer (Bio-Rad Laboratories, Inc., Waltham, MA, USA) at a 450 nm wavelength. Cell viabilities were determined as the percentages relative to the control group.

Measurement of pro-inflammatory mediators. For the estimations of inflammatory responses, the levels of tumor necrosis factor (TNF)-α and interleukin (IL)-6 were determined using commercial ELISA kits (Nanjing Jiancheng Bioengineering Institute) according to the manufacturer's protocols (2).

Apoptotic evaluation using flow cytometry. For apoptotic evaluation, Annexin V-FITC/PI double staining was performed as described previously (14,15). Following experimental treatment, the PC12 cells were collected, washed with PBS and stained using the commercial apoptosis detection kit (Sigma-Aldrich; Merck Millipore) in accordance with the manufacturer's protocol. The PC12 cells ($1x10^6$ cells/ml) were then resuspended in PBS (Gibco; Thermo Fisher Scientific, Inc.) and incubated with 5 μl of PI dye at room temperature for 15 min. Subsequently, 1 μl of Annexin V was added into the cell suspension and maintained for another 15 min shielded from light. Finally, the cells were analyzed by fluorescence-activated cell sorting via flow cytometric analysis (CytoFLEX; Beckman Coulter, Inc., Brea, CA, USA). Cells revealed to stain positively for Annexin V or PI were considered apoptotic cells.

Detection of ROS generation. A DHE fluorescent probe (Beyotime Institute of Biotechnology Co., Ltd., Haimen, China) and flow cytometric assays were performed to determine the generation of ROS in PC12 cells, as in a previously described method (16). In detail, the cells in each group were adjusted to $1.5x10^5$ per well, and seeded into a 24-well plate. Following OGD/R treatment, the medium was removed and a DHE fluorescent probe (10 μmol/l) dissolved in serum-free medium was added to the wells for 30 min at room temperature. Flow cytometry (FACSCalibur; BD Biosciences, Franklin Lakes, NJ, USA) was performed to calculate the DHE-positive ratio.

To further evaluate the intercellular superoxide generation and lipid peroxidation induced by OGD/R, the concentration of malondialdehyde (MDA) and activity of superoxide dismutase (SOD) of the PC12 cells in each group were measured using commercially available kits (Nanjing Jiancheng Bioengineering Institute) in accordance with the manufacturer's protocol (17).

Reverse transcription-quantitative polymerase chain reaction (RT-qPCR) analysis. Total RNA from the treated PC12 cells was extracted using TRIzol (Invitrogen; Thermo Fisher Scientific, Inc.) as previously described (1,2,16). The transcription first strand cDNA synthesis kit (Roche Diagnostics, Basel, Switzerland) was used to synthesize cDNA. The mRNA expression of RP105 was determined by RT-qPCR analysis, which was performed using SYBR-Green PCR Master mix (Roche Diagnostics). The reverse transcriptase product (2 μl) was reacted with the StepOnePlus system (Thermo Fisher Scientific, Inc.) in a mixture (20 μl) containing 0.4 μl of TaKaRa SYBR-Green (Roche Diagnostics), 0.4 mol/l each primer, and 10 μl of SYBR Premix Ex Taq (Roche Diagnostics). Thermocycling conditions were as follows: 50˚C for 2 min, 95˚C for 10 min, and 40 cycles of 95˚C for 30 sec and 60˚C for 30 sec. The results were normalized against the gene expression of β-actin. The $2^{-\Delta\Delta Cq}$ method was used to calculate relative gene expression (14). The primers sequences for the amplification were as follows: RP105, forward 5'-TGA GGGCCTCTGTGAAATGT-3' and reverse, 5'-GGAAGCACT GATTTGGCACA-3'; β-actin, forward 5'-CACGATGGAGGG GCCGGACTCATC-3' and reverse 5'-TAAAGACCTCTA TGCCAACACAGT-3'.

Western blot analysis. The protocols used for western blot analysis have been reported previously (1,2,16). In detail, PC12 cells were washed twice with PBS (Gibco; Thermo Fisher Scientific, Inc.), and were lysed using 200 μl of lysis buffer containing phenylmethylsulfonyl fluoride (1 mM) on ice for 30 min. The lysates were collected with cell scraper, and then centrifuged at 20,000 x g at 4˚C for 5 min. The BCA protein assay kit (Beyotime Institute of Biotechnology) was utilized to determine the concentrations. Extracts containing 40 μg of protein in each group were subjected to 10% SDS-PAGE and transferred onto polyvinylidene fluoride (PVDF) membranes (EMD Millipore, Billerica, MA, USA). The membranes were then blocked with 5% non-fat dried milk dissolved in Tris-buffered saline with 0.1% Tween-20 for 1 h at room temperature. The PVDF membranes were then incubated with primary antibodies targeting RP105 (1:800 dilution; Santa Cruz Biotechnology, Inc., Dallas, TX, USA; cat. no. sc-27841), PI3K (1:1,000 dilution; Cell Signaling Technology, Inc., Danvers, MA, USA; cat. no. 4255), phosphorylated (p-)AKT (Ser473; Cell Signaling Technology, Inc.; cat. no. 4060), AKT (1:1,000 dilution; Cell Signaling Technology, Inc.; cat. no. 9272), p-glycogen synthase kinase 3β (1:2,000 dilution; p-GSK-3β; Abcam, Cambridge, UK; cat. no. ab75745), GSK-3β (1:2,000 dilution; Abcam; cat. no. ab93926), cleaved caspase-9 (1:500 dilution; Abscitech, College Park, MD, USA; cat. no. 40503-1), cleaved caspase-3 (1:2,000 dilution; Abcam; cat. no. ab2302) and GAPDH (1:1,000 dilution; Abcam; cat. no. ab37168) overnight at 4˚C. Subsequently, the blots were incubated with horseradish peroxidase-conjugated rabbit anti-rat IgG secondary antibodies (1:1,000 dilution; cat. no. bs-0346R-HRP; BIOSS, Beijing, China) for 2 h at room temperature. Finally, the target bands were visualized using ECL reagent (Thermo Fisher Scientific, Inc.). The signal intensities were quantified using BandScan 5.0 software (Glyko, Inc., Novato, CA USA), and normalized to GAPDH.

Statistical analysis. All data are expressed as the mean ± standard deviation. Statistical comparisons were performed using one-way analysis of variance followed by Tukey's test for post-hoc analysis, and a Student's t-test for comparisons between two groups. $P<0.05$ was considered to indicate a statistically significant difference. Data and statistical analyses were performed by SPSS 13.0 software (SPSS, Inc., Chicago, IL, USA).

Results

OGD/R leads to the downregulation of RP105 in PC12 cells. To examine the potential effects of RP105 in neuronal OGD/R injury, levels of RP105 were measured following the OGD/R procedure in PC12 cells. Compared with the control group, the expression of RP105 at the protein and mRNA levels was significantly reduced in the OGD/R-treated PC12 cells ($P<0.05$; Fig. 1A and B). Ad-RP105 transduction prior to OGD/R significantly promoted the expression of RP105 in PC12 cells (Ad-RP105+OGD/R, vs. OGD/R group; $P<0.05$), which confirmed the successful transduction of the adenoviral vector. No significant difference was found in the expression of RP105 between the Ad-GFP+OGD/R group and the OGD/R group ($P>0.05$). These findings indicated the possibility that RP105 may be crucial in the neuronal OGD/R process.

Upregulation of RP105 increases cell viability following OGD/R treatment. To estimate whether the overexpression of RP105 affects OGD/R injury, cellular viability and necrotic markers were evaluated using a CCK-8 assay and LDH release detection, respectively. As shown in Fig. 2A, OGD/R induced a significant decrease of cellular viability in the PC12 cells, compared with those in the control group ($P<0.05$). By contrast, Ad-RP105 transduction increased viability, compared with that in the OGD/R group ($P<0.05$). A similar trend was shown in the OGD/R-induced elevation of LDH release (Fig. 2B). A lower concentration of LDH was observed in the Ad-RP105+OGD/R group, compared with that in the OGD/R group ($P<0.05$). Transduction with Ad-GFP had no significant effect on the results of the CCK-8 or LDH assays ($P>0.05$).

Upregulation of RP105 represses OGD/R-induced inflammation, apoptosis and ROS. OGD/R injury is closely associated with the stimulation of inflammation, apoptosis and ROS (1,2,16,17). In the subsequent experiments, the present study investigated the involvement of RP105 in the changes of pro-inflammatory mediators (IL-6 and TNF-α), apoptotic molecules (cleaved caspase-9/-3) and ROS-associated markers (MDA and SOD) during OGD/R of PC12 cells. In addition, a flow cytometer was utilized to quantify apoptosis and ROS. As shown in Fig. 3, minimal concentrations of IL-6 and TNF-α

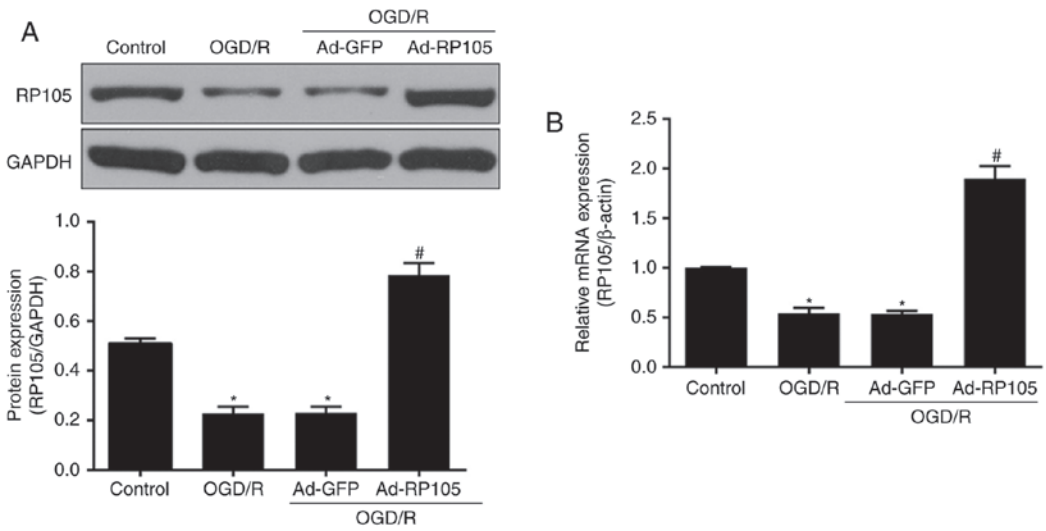

Figure 1. OGD/R leads to the downregulation of RP105 in PC12 cells. (A) Original representative immunoblots and quantitative evaluation of protein levels of RP105 normalized to GAPDH. (B) Quantitative data of RP105 mRNA was detected by reverse transcription-quantitative polymerase chain reaction analysis. Data are expressed as the mean ± standard deviation (n=3). *P<0.05, compared with the control group; #P<0.05, compared with the OGD/R group. OGD/R, oxygen-glucose deprivation/reoxygenation; Ad, adenovirus; RP105, radioprotective 105 kDa protein.

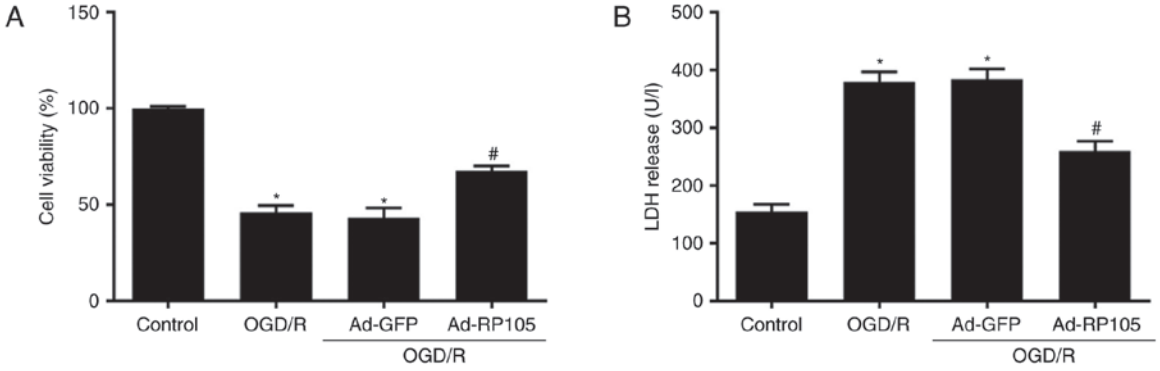

Figure 2. Upregulation of RP105 increases cell viability following OGD/R treatment. (A) Viability of PC12 cells was evaluated using a Cell Counting Kit-8 assay. (B) LDH release into culture medium was measured by ELISA measurement. Data are expressed as the mean ± standard deviation (n=3). *P<0.05, compared with the control group; #P<0.05, compared with the OGD/R group. OGD/R, oxygen-glucose deprivation/reoxygenation; LDH, lactate dehydrogenase; Ad, adenovirus; RP105, radioprotective 105 kDa protein.

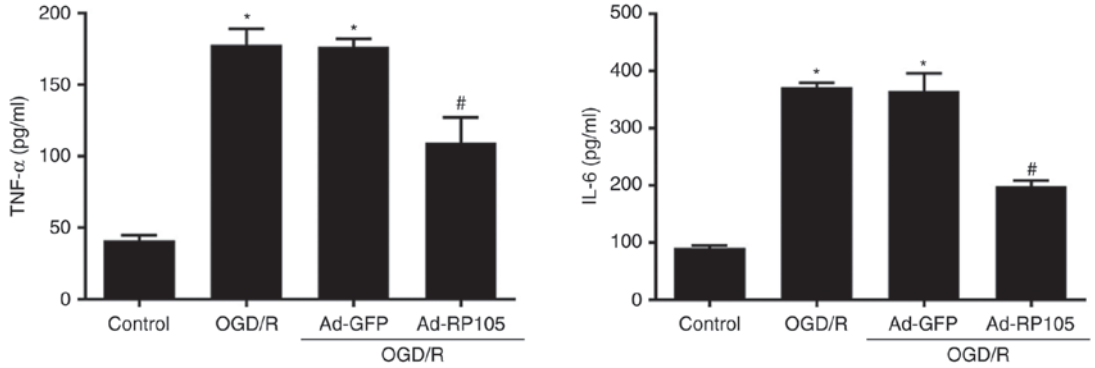

Figure 3. Upregulation of RP105 represses OGD/R-induced inflammation. The levels of pro-inflammatory mediators, including IL-6 and TNF-α, in PC12 cells under OGD/R was detected in culture supernatant by ELISA. Data are expressed as the mean ± standard deviation (n=3). *P<0.05, compared with the control group; #P<0.05, compared with the OGD/R group. OGD/R, oxygen-glucose deprivation/reoxygenation; IL-6, interleukin-6; TNF-α, tumor necrosis factor-α; Ad, adenovirus; RP105, radioprotective 105 kDa protein.

were observed in the control group, whereas OGD/R significantly accelerated inflammatory responses, compared with those in the control group (P<0.05). As expected, the cells in the Ad-RP105 transfection group exhibited lower IL-6/TNF-α

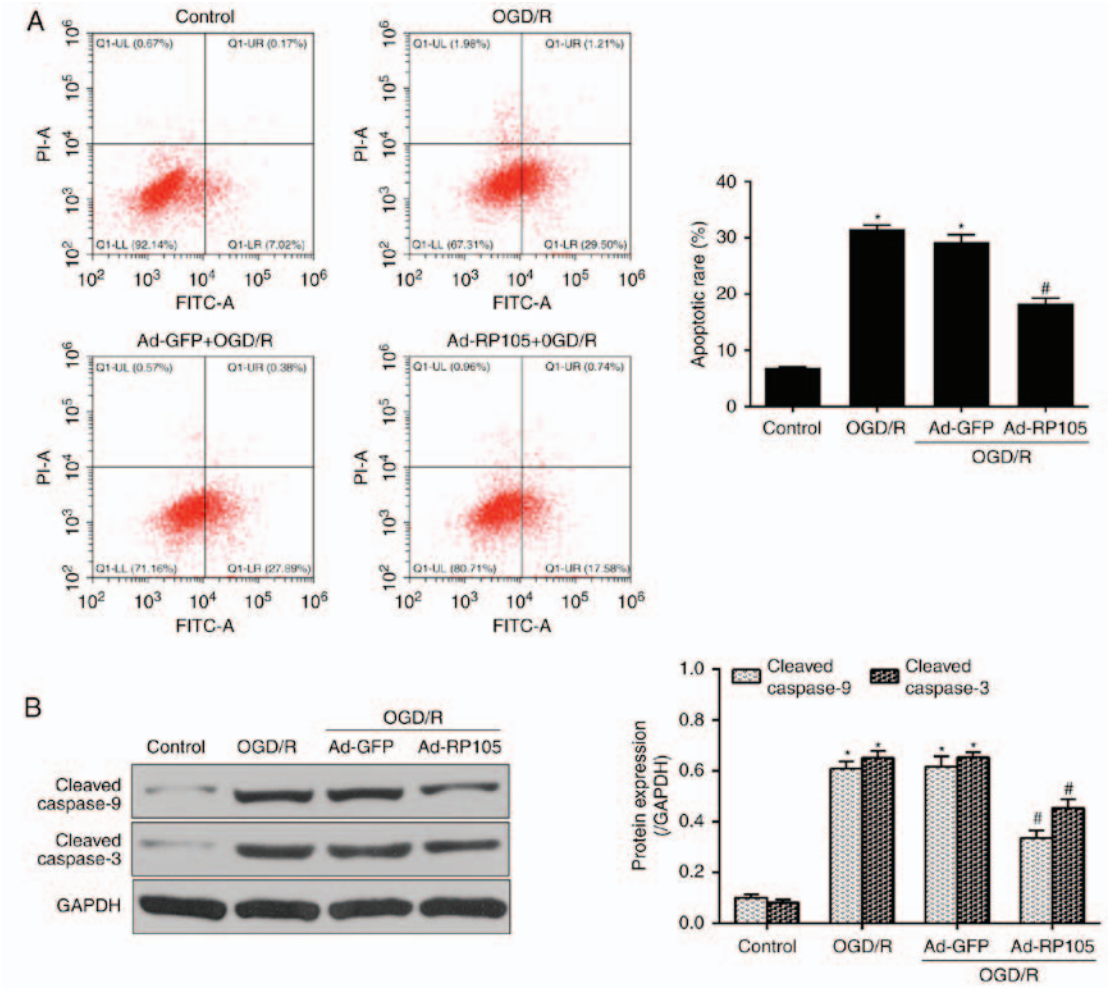

Figure 4. Upregulation of RP105 represses OGD/R-induced apoptosis. (A) Apoptotic cells were detected by flow cytometry, and apoptotic rates included early and late apoptotic events. (B) Protein levels of cleaved caspase-9/-3 were detected by western blot analysis. GAPDH was used as internal control. Data are expressed as the mean ± standard deviation (n=3). *P<0.05, compared with the control group; #P<0.05, compared with the OGD/R group. OGD/R, oxygen-glucose deprivation/reoxygenation; Ad, adenovirus; RP105, radioprotective 105 kDa protein.

release, compared with those in the OGD/R group (P<0.05). Similarly, the OGD/R-induced elevation of apoptosis, as exhibited by increased apoptotic rate (Fig. 4A) and protein expression levels of cle-caspase-9/-3 (Fig. 4B), was reversed by the overexpression of RP105 (Ad-RP105+OGD/R, vs. OGD/R group, P<0.05).

The oxidative status of OGD/R injury on PC12 cells elicited similar patterns. As shown in Fig. 5A, the results from quantitative evaluations of DHE-positive cells using flow cytometry revealed that OGD/R promoted intercellular ROS generation in PC12 cells, compared with those in the control group (P<0.05) and, in contrast Ad-RP105 transduction effectively limited OGD/R-induced ROS (Ad-RP105+OGD/R, vs. OGD/R group, P<0.05). Furthermore, the accumulation of MDA, a by-product of lipid peroxidation, and activity of SOD, an indicator of antioxidant defense, are widely used to reflect oxidative responses to OGD/R injury (Fig. 5B). It was found that OGD/R significantly alleviated the activity of SOD but aggravated the production of MDA, compared with the control group (P<0.05). Following transduction with Ad-RP105, the effects on these two parameters of oxidative stress were reversed, compared with those in the OGD/R group (P<0.05), indicating favorable effects of RP105 against ROS in OGD/R. The cells transduced with Ad-GFP prior to OGD/R exhibited no differences in inflammation, apoptosis or ROS, compared with those in the OGD/R group (P>0.05).

Upregulation of RP105 activates the PI3K/AKT pathways during OGD/R injury. The PI3K/AKT pathway acts as one of the major pro-survival mediators, and its activation is fundamental in decreasing inflammation, apoptosis and ROS in OGD/R-affected PC12 cells (18,19). To detect whether the PI3K/AKT pathway was involved in the OGD/R-inhibitory effects of RP105, the present study examined the expression levels of PI3K/AKT and downstream effector GSK-3β using western blot analysis. As shown in Fig. 6, OGD/R caused marked reductions in the expression of PI3K, and phosphorylation of AKT and GSK-3β, which were upregulated following Ad-RP105 transduction (Ad-RP105+OGD/R, vs. OGD/R group; P<0.05). Ad-GFP treatment had no significant effects on the expression levels of these proteins, compared with levels in the OGD/R group (P>0.05).

Inhibition of the PI3K/AKT pathway eliminates the neuroprotective effects of RP105. In the subsequent investigations, whether the neuroprotective effect of the

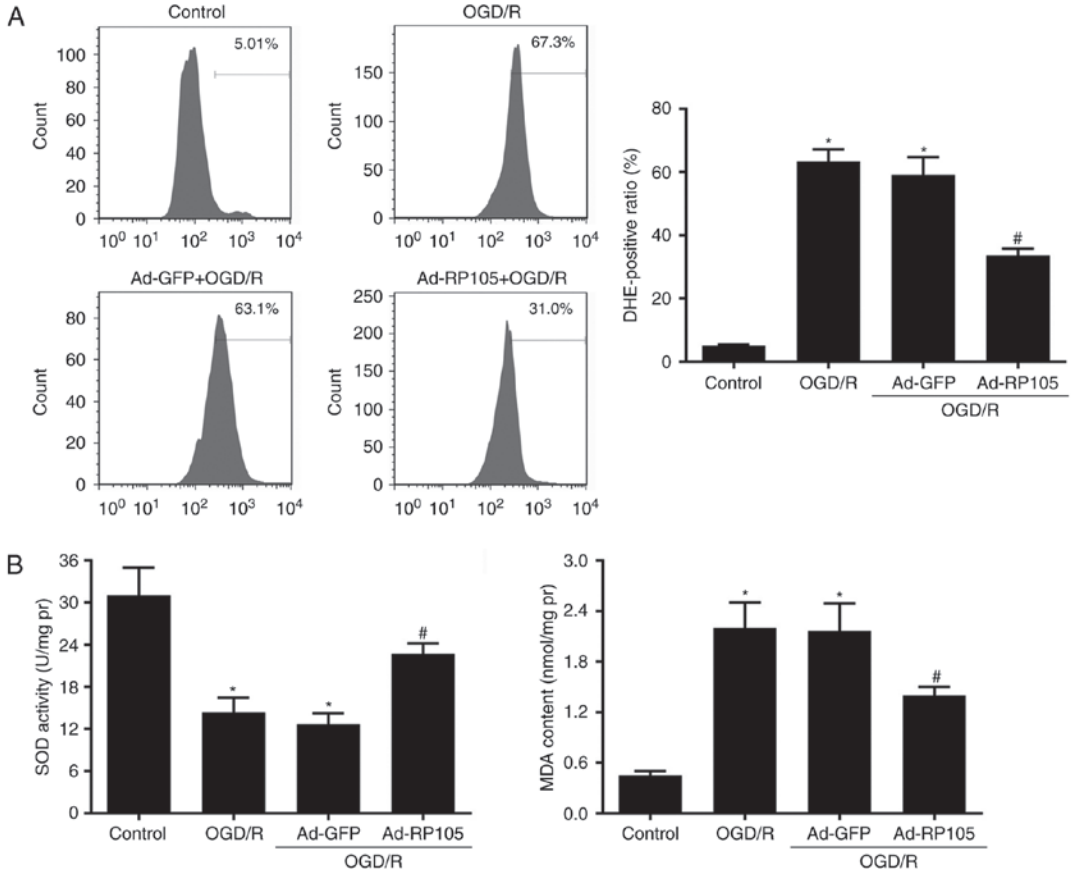

Figure 5. Upregulation of RP105 represses OGD/R-induced ROS. (A) Flow cytometry was performed to quantify ROS accumulation in PC12 cells incubated with DHE probe. (B) MDA content and SOD activity were measured using commercial kits. Data are expressed as the mean ± standard deviation (n=3). *P<0.05, compared with the control group; #P<0.05, compared with the OGD/R group. OGD/R, oxygen-glucose deprivation/reoxygenation; ROS, reactive oxygen species; MDA, malondialdehyde; SOD, superoxide dismutase; Ad, adenovirus; RP105, radioprotective 105 kDa protein.

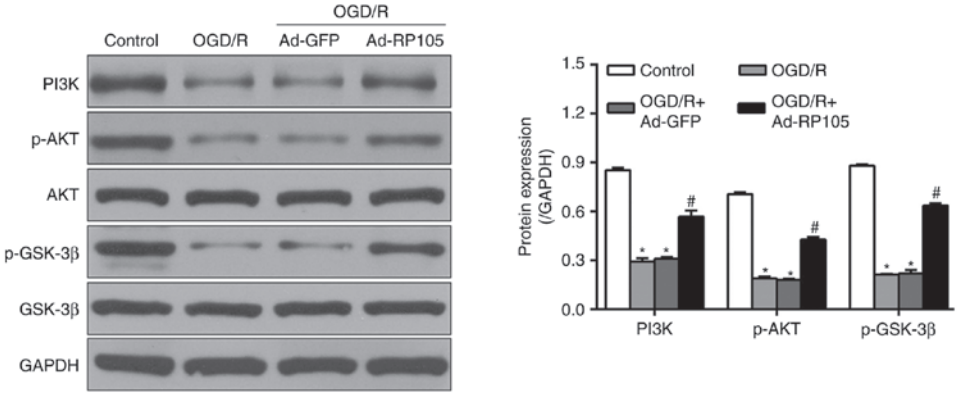

Figure 6. Upregulation of RP105 activates the PI3K/AKT pathways in OGD/R injury. The original immunoblots of PI3K, p-Akt, Akt, GSK-3β and p-GSK-3β, and their corresponding bar graphs of densitometry were measured by western blot analysis. GAPDH was used as internal control. Data are expressed as the mean ± standard deviation (n=3). *P<0.05, compared with the control group; #P<0.05, compared with the OGD/R group. OGD/R, oxygen-glucose deprivation/reoxygenation; PI3K, phosphatidylinositol 3-kinase; AKT, protein kinase B; GSK-3β, glycogen synthase kinase-3β; p-, phosphorylated; Ad, adenovirus; RP105, radioprotective 105 kDa protein.

overexpression of RP105 during OGD/R injury is dependent on the PI3K/AKT-mediated pathways was investigated. The Ad-RP105 and Ad-GFP-transduced PC12 cells were subjected to a specific PI3K/AKT inhibitor (LY294002) or PBS vehicle, followed by OGD/R insult. Cell viability was reduced in the LY294002-treated PC12 cells, compared with the PBS-treated cells following Ad-RP105 transduction during OGD/R insult (Fig. 7A). The administration of LY294002 notably reversed the anti-OGD/R effects of RP105, as indicated by the reinforced LDH activity, and elevated levels of inflammation, apoptosis and ROS (Fig. 7B and C). Of note, the overexpression of RP105 had no effect on these parameters following Ad-GFP transduction in the presence of LY294002 in OGD/R (P>0.05). Together, these findings indicated that there was a

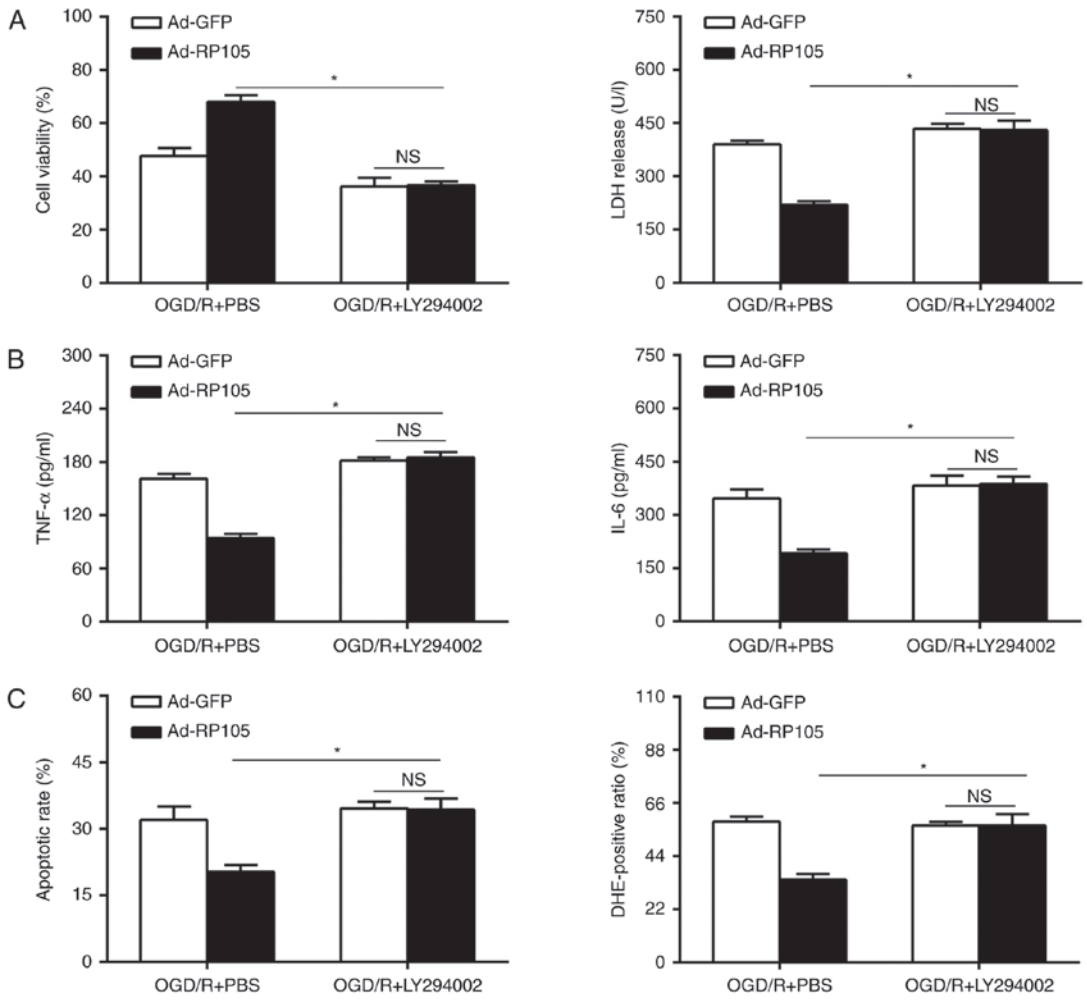

Figure 7. Inhibition of the phosphatidylinositol 3-kinase/protein kinase B pathway eliminated the neuroprotective effects of RP105. (A) Cell viability and LDH release were detected using a Cell Counting Kit-8 and ELISA assays, respectively. (B) Levels of IL-6 and TNF-α in culture medium were estimated via ELISA assays. (C) Cell apoptosis and ROS were examined via flow cytometry. Data are expressed as the mean ± standard deviation (n=3). *P<0.05, compared with the OGD/R+PBS+Ad-RP105 group. OGD/R, oxygen-glucose deprivation/reoxygenation; LDH, lactate dehydrogenase; IL-6, interleukin-6; TNF-α, tumor necrosis factor-α; Ad, adenovirus; RP105, radioprotective 105 kDa protein; NS, no significant difference.

RP105-PI3K-AKT survival axis in the OGD/R paradigm, and that RP105 ameliorated cerebral I/R injury, at least in part, by activating the PI3K/AKT signaling pathway.

Discussion

The present study demonstrated that the overexpression of RP105 serves as an approach to generate anti-OGD/R effects in PC12 cells. The following evidence confirmed this hypothesis: i) Adenoviral transduction followed by OGD/R contributed to the overexpression of RP105 in PC12 cells; ii) overexpression of RP105 prior to OGD/R markedly promoted cell survival, and reduced inflammation, apoptosis and ROS; iii) mechanistic evaluations suggested that RP105 triggered the PI3K/AKT pro-survival signaling pathway in the OGD/R condition, which was confirmed by the fact that PI3K/AKT inhibition eliminated the neuroprotective effects yielded by RP105 reinforcement in PC12 cells. Taken together, these results indicated that RP105 may be a potential target for attenuating neuronal OGD/R injury.

Due to a lack of direct extracellular ligands, transmembrane receptor RP105, as one of the pivotal mediators in intercellular cascade events including apoptosis and inflammation, elicited multiple pathological functions via functional and structural connections with its homology TLRs (9-11). For example, Yang *et al* (6) reported that RP105 protected the myocardium from I/R injury by inhibiting the TLR4/P38 mitogen-activated protein kinase (MAPK)/activator protein-1-mediated mitochondrial apoptotic cascades. Its anti-inflammatory property was also verified in their following investigations; as expected, the molecular mechanisms were, at least in part, due to the limitation of TLR4/nuclear factor (NF)-κB-induced inflammation (20,21). Similarly, Xiong *et al* (5) highlighted the involvement of RP105 in pressure overload-induced cardiac remodeling, in which RP105 markedly inhibited the expression of pro-inflammatory mediators, including MAPK kinase-extracellular signal-regulated kinase 1/2 and NF-κB, through a cooperative pattern with the secreted protein myeloid differentiation-1. These results indicate the potential of RP105 as a common therapeutic target against cardiovascular diseases. However, intervention with RP105 through TLR4-dependent pathways appeared to be unable to reduce I/R or hypertrophy, which suggested that there may exist unrecognized modulatory models independent of TLR4.

In the present study, it was confirmed that the activity of the RP105-PI3K-AKT axis acted as an important pro-survival mechanism in neuronal OGD/R injury. Therefore, the data obtained expands on the beneficial characteristics of RP105 to include the treatment of cerebral I/R disorder in addition to cardiovascular disease and, more prospectively, confirmed the previously undefined mechanism beyond TLR4-associated mechanisms.

Consistent with the present study, investigations have focused increased attention on the TLR4-independent functions of RP105, which appear to improve its regulatory networks (10,12). Among these, the facilitated vein lesions in RP105$^{-/-}$ mice have been associated with an increased level of chemoattractant chemokine (C-C motif) ligand-2 (22). The loss of RP105 has been shown to alleviate atherosclerotic performance through reducing C-C chemokine receptor-2 (23). In addition, RP105 serves as a pro-inflammatory regulator in adipose tissue independent of TLR4 (24). In addition to direct or indirect pathways mediated by RP105, results showing a physical connection between RP105 and PI3K have attracted interest. Yu *et al* (12) revealed that p110δ, as the catalytic subunit of PI3K, was a potent downstream effector reliant on RP105. It was suggested that Bruton's tyrosine kinase acted as one of the tyrosine residues of RP105 in the cytoplasmic tail, which physically linked RP105 with PI3K (12). In this manner, it functioned as an essential adaptor in inducing RP105-dependent stimulations of PI3K and AKT. Based on the above, the present study hypothesized that there may be functional associations between RP105 and the PI3K/AKT axis. As expected, the association between the RP105-PI3K-AKT axis and neuroprotective benefits was confirmed in OGD/R-exposed PC12 cells in the present study. This was also indicated by the adverse effects observed from the inhibition of PI3K/AKT. Further investigations may be required to verify whether other molecular mechanisms are involved in RP105-induced pleiotropic protection against cerebral I/R injury.

The PI3K/AKT axis is a well-known pro-survival mediator, and is commonly regarded as an upstream negative mediator of inflammation, apoptosis and ROS in cerebral I/R injury (17,18,25). The AKT-mediated phosphorylation of GSK-3β at Ser9, and its subsequent inactivation, function as a pivotal switch in regulating multiple protective genes that are responsible for resistance to cerebral I/R injury (2). In accordance with this concept, the present study confirmed that the activation of PI3K/AKT in an RP105-dependent manner reversed the OGD/R-induced damage to PC12 cells, accompanied by weakened inflammation, apoptosis and ROS. Notably, it was increasingly clear that PI3K/AKT acted as a direct downstream effector of RP105, and that the increase of RP105 resulted in higher levels of PI3K, p-AKT and p-GSK-3β. In addition, by applying PI3K/AKT inhibitor, the anti-OGD/R benefits rendered by RP105 were markedly inhibited. In combination with the above data, the results of the present study reinforced the neuroprotective potency of RP105 against I/R injury, specifically regarding modulation of the PI3K/AKT/GSK-3β pathway.

In conclusion, the present study demonstrated that RP105 was an intrinsic positive mediator of cerebral I/R injury via interference of inflammation, apoptosis and ROS. The RP105-PI3K-AKT axis provides an appealing target for cerebral I/R treatment. Of note, further investigations are urgently required to identify possible molecules, particularly microRNAs and long non-coding RNAs, which directly target the RP105-PI3K-AKT axis, and may offer novel understanding and innovate therapeutic strategies for cerebral I/R injury.

Acknowledgements

This study was supported by the National Natural Science Foundation of China (grant no. 81671238).

Competing interests

The authors declare that they have no competing interests.

References

1. Wang N, Zhang L, Lu Y, Zhang M, Zhang Z, Wang K and Lv J: Down-regulation of microRNA-142-5p attenuates oxygen-glucose deprivation and reoxygenation-induced neuron injury through up-regulating Nrf2/ARE signaling pathway. Biomed Pharmacother 89: 1187-1195, 2017.
2. Zhang JF, Zhang L, Shi LL, Zhao ZH, Xu H, Liang F, Li HB, Zhao Y, Xu X, Yang K and Tian YF: Parthenolide attenuates cerebral ischemia/reperfusion injury via Akt/GSK-3β pathway in PC12 cells. Biomed Pharmacother 89: 1159-1165, 2017.
3. Jian Z, Ding S, Deng H, Wang J, Yi W, Wang L, Zhu S, Gu L and Xiong X: Probenecid protects against oxygen-glucose deprivation injury in primary astrocytes by regulating inflammasome activity. Brain Res 1643: 123-129, 2016.
4. Li X, Yang J, Yang J, Dong W, Li S, Wu H and Li L: RP105 protects against myocardial ischemia-reperfusion injury via suppressing TLR4 signaling pathways in rat model. Exp Mol Pathol 100: 281-286, 2016.
5. Xiong X, Liu Y, Mei Y, Peng J, Wang Z, Kong B, Zhong P, Xiong L, Quan D, Li Q, *et al*: Novel protective role of myeloid differentiation 1 in pathological cardiac remodeling. Sci Rep 7: 41857, 2017.
6. Yang J, Guo X, Yang J, Ding JW, Li S, Yang R, Fan ZX and Yang CJ: RP105 protects against apoptosis in ischemia/reperfusion-induced myocardial damage in rats by suppressing TLR4-mediated signaling pathways. Cell Physiol Biochem 36: 2137-2148, 2015.
7. Wang Y, Chen G, Yu X, Li Y, Zhang L, He Z, Zhang N, Yang X, Zhao Y, Li N and Qiu H: Salvianolic acidB ameliorates cerebral ischemia/reperfusion injury through inhibiting TLR4/MyD88 signaling pathway. Inflammation 39: 1503-1513, 2016.
8. Tao X, Sun X, Yin L, Han X, Xu L, Qi Y, Xu Y, Li H, Lin Y, Liu K and Peng J: Dioscin ameliorates cerebral ischemia/reperfusion injury through the downregulation of TLR4 signaling via HMGB-1 inhibition. Free Radic Biol Med 84: 103-115, 2015.
9. Louwe MC, Karper JC, de Vries MR, Nossent AY, Bastiaansen AJ, van der Hoorn JW, Willems van Dijk K, Rensen PC, Steendijk P, Smit JW and Quax PH: RP105 deficiency aggravates cardiac dysfunction after myocardial infarction in mice. Int J Cardiol 176: 788-793, 2014.
10. Guo X, Jiang H and Chen J: RP105-PI3K-Akt axis: A potential therapeutic approach for ameliorating myocardial ischemia/reperfusion injury. Int J Cardiol 206: 95-96, 2016.
11. J Peng Y, Liu X, Xiong X, Huang C, Mei Y, Wang Z, Tang Y, Ye J, Kong B, Liu W, *et al*: Loss of MD1 exacerbates pressure overload-induced left ventricular structural and electrical remodelling. Sci Rep 7: 5116, 2016.
12. CH Yu, Micaroni M, Puyskens A, Schultz TE, Yeo JC, Stanley AC, Lucas M, Kurihara J, Dobos KM, Stow JL and Blumenthal A: RP105 engages phosphatidylinositol 3-kinase p110δ to facilitate the trafficking and secretion of cytokines in macrophages during mycobacterial infection. J Immunol 195: 3890-3900, 2015.
13. Wang Y, Zhang J, Han M, Liu B, Gao Y, Ma P, Zhang S, Zheng Q and Song X: SMND-309 promotes neuron survival through the activation of the PI3K/Akt/CREB-signalling pathway. Pharm Biol 54: 1982-1990, 2016.

14. Yang J, Chen L, Ding J, Zhang J, Fan Z, Yang C, Yu Q and Yang J: Cardioprotective effect of miRNA-22 on hypoxia/reoxygenation induced cardiomyocyte injury in neonatal rats. Gene 579: 17-22, 2016.
15. Yang J, Chen L, Ding J, Fan Z, Li S, Wu H, Zhang J, Yang C, Wang H, Zeng P and Yang J: MicroRNA-24 inhibits high glucose-induced vascular smooth muscle cell proliferation and migration by targeting HMGB1. Gene 586: 268-273, 2016.
16. Xu J, Hua C, Pan X, Fu X and Wu W: Eupatilin inhibits OGD/R-induced neuronal injury in PC12 cells. Int J Clin Exp Med 10: 6728-6734, 2017.
17. Liu X, Zhu X, Chen M, Ge Q, Shen Y and Pan S: Resveratrol protects PC12 cells against OGD/R-induced apoptosis via the mitochondrial-mediated signaling pathway. Acta Biochim Biophys Sin 48: 342-353, 2016.
18. Luo T, Liu G, Ma H, Lu B, Xu H, Wang Y, Wu J, Ge P and Liang J: Inhibition of autophagy via activation of PI3K/Akt pathway contributes to the protection of ginsenoside Rb1 against neuronal death caused by ischemic insults. Int J Mol Sci 15: 15426-15442, 2014.
19. Choi HS, Kim MK, Choi YK, Shin YC, Cho SG and Ko SG: Rhus verniciflua Stokes (RVS) and butein induce apoptosis of paclitaxel-resistant SKOV-3/PAX ovarian cancer cells through inhibition of AKT phosphorylation. BMC Complement Altern Med 16: 122, 2016.
20. Guo X, Jiang H, Yang J, Chen J, Yang J, Ding JW, Li S, Wu H and Ding HS: Radioprotective 105 kDa protein attenuates ischemia/reperfusion-induced myocardial apoptosis and autophagy by inhibiting the activation of the TLR4/NF-κB signaling pathway in rats. Int J Mol Med 38: 885-893, 2016.
21. Yu Q, Yang J, Dong W, Li X, Guo X and Yang R: Increased expression of RP105 decreases cardiomyocytes hypoxia/reoxygenation injury through the TLR4/NF-κB signaling pathway. Int J Clin Exp Pathol 9: 960-968, 2016.
22. Wezel A, de Vries MR, Maassen JM, Kip P, Peters EA, Karper JC, Kuiper J, Bot I and Quax PH: Deficiency of the TLR4 analogue RP105 aggravates vein graft disease by inducing a pro-inflammatory response. Sci Rep 6: 24248, 2016.
23. Wezel A, van der Velden D, Maassen JM, Lagraauw HM, de Vries MR, Karper JC, Kuiper J, Bot I and Quax PH: RP105 deficiency attenuates early atherosclerosis via decreased monocyte influx in a CCR2 dependent manner. Atherosclerosis 238: 132-139, 2015.
24. Nagai Y, Watanabe Y and Takatsu K: The TLR family protein RP105/MD-1 complex: A new player in obesity and adipose tissue inflammation. Adipocyte 2: 61-66, 2013.
25. Jiao S, Zhu H, He P and Teng J: Betulinic acid protects against cerebral ischemia/reperfusion injury by activating the PI3K/Akt signaling pathway. Biomed Pharmacother 84: 1533-1537, 2016.